

Published in final edited form as:

*Bioorg Med Chem Lett.* 2014 January 1; 24(1): 195–198. doi:10.1016/j.bmcl.2013.11.042.

## Linker modification reduced the renal uptake of technetium-99m-labeled Arg-Ala-Asp-conjugated alpha-melanocyte stimulating hormone peptide

Jianquan Yang<sup>a</sup>, Adam M. Flook<sup>a</sup>, Changjian Feng<sup>a</sup>, and Yubin Miao<sup>a,b,c,\*</sup>

<sup>a</sup>College of Pharmacy, University of New Mexico, Albuquerque, New Mexico 87131, USA

<sup>b</sup>Cancer Research and Treatment Center, University of New Mexico, Albuquerque, New Mexico 87131, USA

<sup>c</sup>Department of Dermatology, University of New Mexico, Albuquerque, New Mexico 87131, USA

### Abstract

The purpose of this study was to examine the biodistribution of <sup>99m</sup>Tc-RAD-Arg-(Arg<sup>11</sup>)CCMSH in B16/F1 melanoma-bearing C57 mice to determine whether the replacement of the Lys linker with an Arg linker could decrease the renal uptake of <sup>99m</sup>Tc-RAD-Arg-(Arg<sup>11</sup>)CCMSH. <sup>99m</sup>Tc-RAD-Arg-(Arg<sup>11</sup>)CCMSH exhibited rapid and high tumor uptake (17.98 ± 4.96% ID/g at 2 h post-injection) in B16/F1 melanoma-bearing C57 mice. As compared to <sup>99m</sup>Tc-RAD-Lys-(Arg<sup>11</sup>)CCMSH, the replacement of the Lys linker with an Arg linker dramatically decreased the renal uptake of <sup>99m</sup>Tc-RAD-Arg-(Arg<sup>11</sup>)CCMSH by 68, 62, 73 and 64% at 0.5, 2, 4 and 24 h post-injection, respectively. Flank B16/F1 melanoma lesions were clearly imaged at 2 h post-injection using <sup>99m</sup>Tc-RAD-Arg-(Arg<sup>11</sup>)CCMSH as an imaging probe.

### Keywords

Alpha-melanocyte stimulating hormone peptide; melanocortin-1 receptor; renal uptake; melanoma imaging

Melanocortin-1 (MC1) receptor is a G protein-coupled receptor which is over-expressed on human and mouse melanoma cells.<sup>1–5</sup> Over the past several years, we have been developing a novel class of radiolabeled alpha-melanocyte stimulating hormone (α-MSH) peptides to target MC1 receptors for melanoma imaging.<sup>5–8</sup> Specifically, the cyclic RXD {Arg-X-Asp-<sup>D</sup>Tyr-Asp} motif (X = Gly, Ala, Ser, Val, Thr, Nle, Phe or <sup>D</sup>Phe) was conjugated to [Cys<sup>3,4,10</sup>, <sup>D</sup>-Phe<sup>7</sup>, Arg<sup>11</sup>]α-MSH<sub>3–13</sub> {(Arg<sup>11</sup>)CCMSH} peptide via a lysine linker to generate a series of RXD-Lys-(Arg<sup>11</sup>)CCMSH peptides. Interestingly, single amino acid at the X position displayed a profound effect in melanoma targeting and clearance properties. First of all, we found that the switch from RGD to RAD dramatically improved the MC1 receptor binding affinity of RAD-Lys-(Arg<sup>11</sup>)CCMSH as compared to RGD-Lys-(Arg<sup>11</sup>)CCMSH in M21 and B16/F1 melanoma cells.<sup>5,6</sup> The stronger MC1 receptor binding

© 2013 Elsevier Ltd. All rights reserved.

**Corresponding Author:** Yubin Miao, 2502 Marble NE, MSC09 5360, College of Pharmacy, University of New Mexico, Albuquerque, NM 87131. Phone: (505) 925-4437; Fax: (505) 272-6749; ymiao@salud.unm.edu.

**Publisher's Disclaimer:** This is a PDF file of an unedited manuscript that has been accepted for publication. As a service to our customers we are providing this early version of the manuscript. The manuscript will undergo copyediting, typesetting, and review of the resulting proof before it is published in its final citable form. Please note that during the production process errors may be discovered which could affect the content, and all legal disclaimers that apply to the journal pertain.

yielded higher melanoma uptake for  $^{99m}\text{Tc}$ -RAD-Lys-(Arg<sup>11</sup>)CCMSH than  $^{99m}\text{Tc}$ -RGD-Lys-(Arg<sup>11</sup>)CCMSH.<sup>6</sup> Moreover, the residues of Ser, Val and Thr resulted in more favorable melanoma targeting and clearance properties than the residues of Nle, Phe or  $\text{D}$ -Phe.<sup>7,8</sup> However, all  $^{99m}\text{Tc}$ -RXD-Lys-(Arg<sup>11</sup>)CCMSH peptides exhibited high non-specific renal uptake. Thus, it is desirable to reduce the renal uptake to facilitate their potential applications.

Despite the profound effect of single amino acid (Gly, Ala, Ser, Val and Thr) at the X position in  $^{99m}\text{Tc}$ -RXD-Lys-(Arg<sup>11</sup>)CCMSH peptides, the positively-charged amino acid residues were same among the  $^{99m}\text{Tc}$ -RXD-Lys-(Arg<sup>11</sup>)CCMSH peptides. Specifically, each  $^{99m}\text{Tc}$ -RXD-Lys-(Arg<sup>11</sup>)CCMSH peptide has three arginine residues and one lysine linker. In our previous reports, *L*-lysine co-injection successfully reduced the renal uptake of  $^{99m}\text{Tc}$ -RXD-Lys-(Arg<sup>11</sup>)CCMSH peptides by 37–55% at 2 h post-injection.<sup>6–8</sup> Meanwhile, it was reported that the replacement of Lys with an Arg dramatically decreased the renal uptake of  $^{99m}\text{Tc}$ -(Arg<sup>11</sup>)CCMSH and  $^{99m}\text{Tc}$ -RGD-Arg-(Arg<sup>11</sup>)CCMSH by 41–64% at 2 h post-injection.<sup>9–11</sup> Therefore, we hypothesized that the replacement of the Lys linker with an Arg linker would decrease the renal uptake of  $^{99m}\text{Tc}$ -RXD-Lys-(Arg<sup>11</sup>)CCMSH peptides. Thus, as a proof-of-principal study, we prepared and evaluated the biodistribution property of  $^{99m}\text{Tc}$ -RAD-Arg-(Arg<sup>11</sup>)CCMSH to examine our hypothesis in this study.

Firstly, RAD-Arg-(Arg<sup>11</sup>)CCMSH was synthesized using fluorenylmethyloxycarbonyl (Fmoc) chemistry, purified by reverse phase-high performance liquid chromatography (RP-HPLC) and characterized by electrospray ionization mass spectrometry according to our published procedure.<sup>12</sup> The schematic structure of RAD-Arg-(Arg<sup>11</sup>)CCMSH is presented in Figure 1. The competitive binding study of RAD-Arg-(Arg<sup>11</sup>)CCMSH was determined in B16/F1 melanoma cells. The competitive binding curve of RAD-Arg-(Arg<sup>11</sup>)CCMSH is presented in Figure 2. The MC1 receptor binding affinity of RAD-Arg-(Arg<sup>11</sup>)CCMSH was 0.22 nM which was comparable to that of RAD-Lys-(Arg<sup>11</sup>)CCMSH (0.26 nM) in B16/F1 cells. The receptor binding result indicated that the replacement of the Lys linker with an Arg linker retained its nanomolar MC1 receptor binding affinity.  $^{99m}\text{Tc}$ -RAD-Lys-(Arg<sup>11</sup>)CCMSH was readily prepared with greater than 95% radiolabeling yield and was separated from its excess nonlabeled peptide by high performance liquid chromatography (HPLC). The radiochemical purity of  $^{99m}\text{Tc}$ -RAD-Lys-(Arg<sup>11</sup>)CCMSH was greater than 98%. The specific activity of  $^{99m}\text{Tc}$ -RAD-Lys-(Arg<sup>11</sup>)CCMSH was  $8.406 \times 10^9$  MBq/g.

Secondly, cellular internalization and efflux properties of  $^{99m}\text{Tc}$ -RAD-Arg-(Arg<sup>11</sup>)CCMSH were examined in B16/F1 melanoma cells. The cellular results are presented in Figure 3.  $^{99m}\text{Tc}$ -RAD-Arg-(Arg<sup>11</sup>)CCMSH exhibited rapid cellular internalization and extended cellular retention. Approximately  $77.81 \pm 4.46\%$  of the  $^{99m}\text{Tc}$ -RAD-Arg-(Arg<sup>11</sup>)CCMSH activity internalized at 20 min post incubation, whereas  $81.26 \pm 4.81\%$  of the  $^{99m}\text{Tc}$ -RAD-Arg-(Arg<sup>11</sup>)CCMSH activity internalized after 2 h incubation. The efflux results demonstrated that  $72.07 \pm 1.61\%$  of the  $^{99m}\text{Tc}$ -RGD-Arg-(Arg<sup>11</sup>)CCMSH activity remained inside the cells 2 h after incubating cells in culture medium.  $^{99m}\text{Tc}$ -RAD-Arg-(Arg<sup>11</sup>)CCMSH displayed similar rapid internalization and extended retention pattern as  $^{99m}\text{Tc}$ -RAD-Lys-(Arg<sup>11</sup>)CCMSH.<sup>11</sup>

Thirdly, the melanoma targeting and pharmacokinetic properties of  $^{99m}\text{Tc}$ -RAD-Arg-(Arg<sup>11</sup>)CCMSH were determined in B16/F1 melanoma-bearing C57 mice. The biodistribution results are presented in Table 1.  $^{99m}\text{Tc}$ -RAD-Arg-(Arg<sup>11</sup>)CCMSH exhibited rapid and high tumor uptake in melanoma-bearing mice. The tumor uptake was  $17.98 \pm 4.96$  and  $14.07 \pm 2.90\%$  ID/g at 2 and 4 h post-injection. In peptide blocking study, approximately 87% of the tumor uptake of  $^{99m}\text{Tc}$ -RAD-Arg-(Arg<sup>11</sup>)CCMSH was blocked

by 10  $\mu\text{g}$  (6.1 nmol) of non-radiolabeled NDP-MSH at 2 h post-injection ( $p < 0.05$ ), demonstrating that the tumor uptake was specific and MC1 receptor-mediated. Whole-body clearance of  $^{99\text{m}}\text{Tc}$ -RGD-Arg-(Arg<sup>11</sup>)CCMSH was rapid, with approximately 75% of the injected radioactivity cleared through the urinary system by 2 h post-injection (Table 1). Normal organ uptake of  $^{99\text{m}}\text{Tc}$ -RGD-Arg-(Arg<sup>11</sup>)CCMSH was generally lower than 1.9% ID/g except for kidneys after 2 h post-injection. High tumor/blood and tumor/muscle uptake ratios were demonstrated as early as 0.5 h post-injection (Table 1). The renal uptake of  $^{99\text{m}}\text{Tc}$ -RAD-Arg-(Arg<sup>11</sup>)CCMSH reached its highest value of  $41.24 \pm 4.48\%$  ID/g at 0.5 h post-injection and decreased to  $11.99 \pm 2.29\%$  ID/g at 24 h post-injection. In peptide blocking study at 2 h post-injection, the renal uptake was not significantly ( $p = 0.063$ ) different with or without the peptide blockade, suggesting that the renal uptake was not receptor-mediated.

As compared to  $^{99\text{m}}\text{Tc}$ -RAD-Lys-(Arg<sup>11</sup>)CCMSH,<sup>11</sup>  $^{99\text{m}}\text{Tc}$ -RAD-Arg-(Arg<sup>11</sup>)CCMSH exhibited comparable melanoma uptake at 2, 4 and 24 h post-injection. The comparable melanoma uptake between  $^{99\text{m}}\text{Tc}$ -RAD-Arg-(Arg<sup>11</sup>)CCMSH and  $^{99\text{m}}\text{Tc}$ -RAD-Lys-(Arg<sup>11</sup>)CCMSH was attributed to the similar receptor binding affinities between RAD-Arg-(Arg<sup>11</sup>)CCMSH and RAD-Lys-(Arg<sup>11</sup>)CCMSH (0.22 vs. 0.26 nM). Despite that  $^{99\text{m}}\text{Tc}$ -RAD-Arg-(Arg<sup>11</sup>)CCMSH and  $^{99\text{m}}\text{Tc}$ -RAD-Lys-(Arg<sup>11</sup>)CCMSH displayed similar distribution pattern in normal organs, the renal uptake of  $^{99\text{m}}\text{Tc}$ -RAD-Arg-(Arg<sup>11</sup>)CCMSH was dramatically lower than that of  $^{99\text{m}}\text{Tc}$ -RAD-Lys-(Arg<sup>11</sup>)CCMSH. The renal uptake of  $^{99\text{m}}\text{Tc}$ -RAD-Lys-(Arg<sup>11</sup>)CCMSH was 3.1, 2.6, 3.7 and 2.8 times the renal uptake of  $^{99\text{m}}\text{Tc}$ -RAD-Arg-(Arg<sup>11</sup>)CCMSH at 0.5, 2, 4 and 24 h post-injection, respectively. The comparable melanoma uptake and dramatically decreased renal uptake of  $^{99\text{m}}\text{Tc}$ -RAD-Arg-(Arg<sup>11</sup>)CCMSH resulted in higher tumor to kidney uptake ratios as compared to  $^{99\text{m}}\text{Tc}$ -RAD-Lys-(Arg<sup>11</sup>)CCMSH.

Finally, the melanoma imaging property of  $^{99\text{m}}\text{Tc}$ -RAD-Arg-(Arg<sup>11</sup>)CCMSH was examined in a B16/F1 melanoma-bearing C57 mouse in this study. The representative whole-body single photon emission computed tomography (SPECT)/CT image is presented in Figure 4. Flank melanoma tumors were visualized clearly by  $^{99\text{m}}\text{Tc}$ -RAD-Arg-(Arg<sup>11</sup>)CCMSH at 2 h post-injection.  $^{99\text{m}}\text{Tc}$ -RAD-Arg-(Arg<sup>11</sup>)CCMSH exhibited high tumor to normal organ uptake ratios except for kidney, which was consistent with the biodistribution results (Table 1). The urine collected from the imaging mouse was analyzed for the metabolites by HPLC. The urinary HPLC profile of  $^{99\text{m}}\text{Tc}$ -RAD-Arg-(Arg<sup>11</sup>)CCMSH is shown in Figure 6.  $^{99\text{m}}\text{Tc}$ -RAD-Arg-(Arg<sup>11</sup>)CCMSH remained intact at 2 h post-injection.

In conclusion, the replacement of the Lys linker with an Arg linker dramatically decreased the renal uptake of  $^{99\text{m}}\text{Tc}$ -RAD-Arg-(Arg<sup>11</sup>)CCMSH while retaining its high melanoma uptake. B16/F1 melanoma lesions were clearly visualized by SPECT/CT using  $^{99\text{m}}\text{Tc}$ -RAD-Arg-(Arg<sup>11</sup>)CCMSH as an imaging probe. High melanoma uptake and decreased renal uptake of  $^{99\text{m}}\text{Tc}$ -RAD-Arg-(Arg<sup>11</sup>)CCMSH suggests that the replacement of the Lys linker with an Arg linker may be useful in reducing the renal uptake of other  $^{99\text{m}}\text{Tc}$ -RXD-Lys-(Arg<sup>11</sup>)CCMSH peptides in future studies.

The experimental details are presented in References and notes.<sup>13–16</sup>

## Acknowledgments

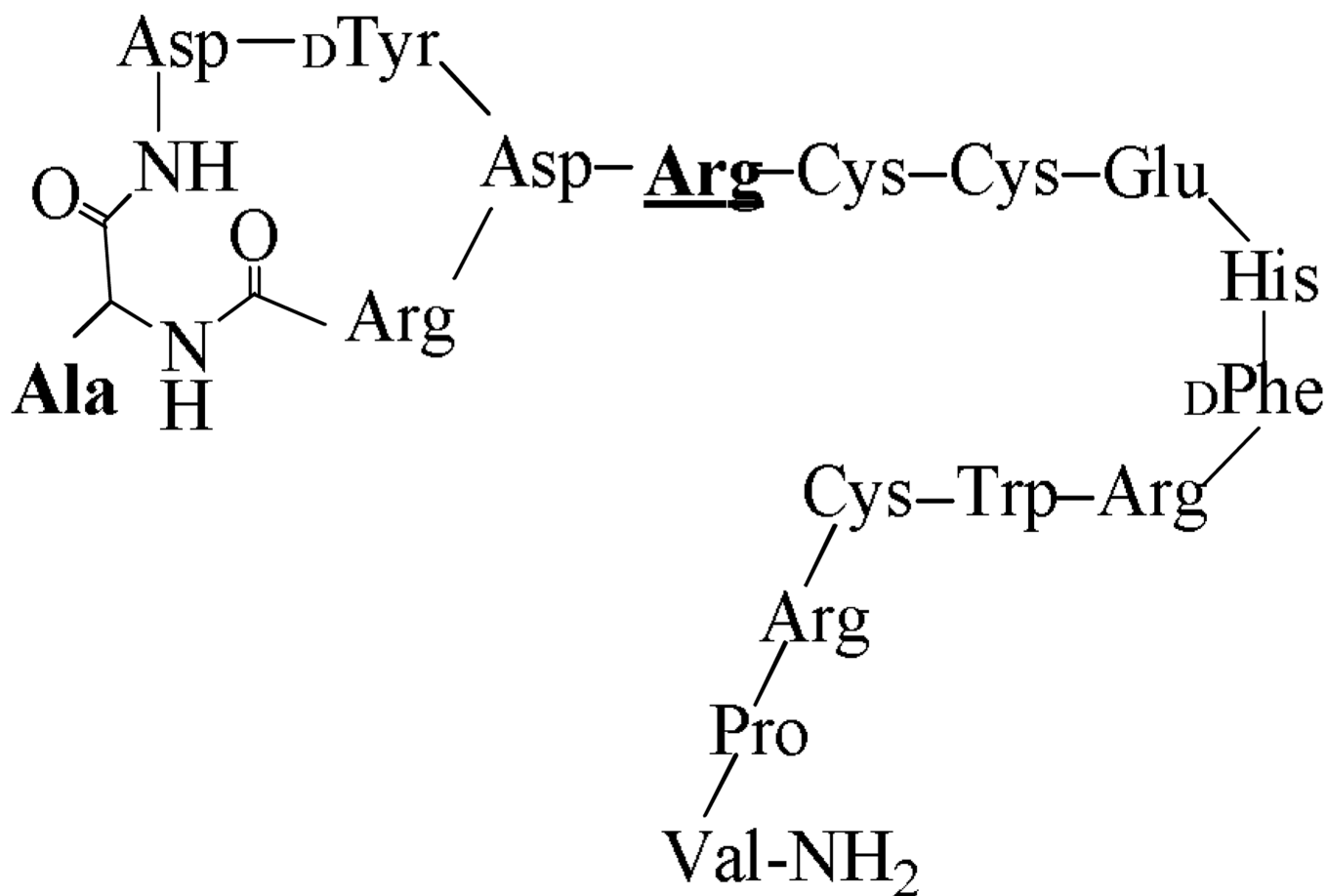
We appreciate Dr. Fabio Gallazzi for his technical assistance. This work was supported in part by the NIH grant NM-INBRE P20RR016480 and the University of New Mexico RAC Award. The image in this article was generated by the Keck-UNM Small Animal Imaging Resource established with funding from the W.M. Keck Foundation and the University of New Mexico Cancer Research and Treatment Center (NIH P30 CA118100).

## References and notes

1. Siegrist W, Solca F, Stutz S, Giuffre L, Carrel S, Girard J, Eberle AN. *Cancer Res.* 1989; 49:6352. [PubMed: 2804981]
2. Tatro JB, Reichlin S. *Endocrinology.* 1987; 121:1900. [PubMed: 2822378]
3. Miao Y, Whitener D, Feng W, Owen NK, Chen J, Quinn TP. *Bioconjug. Chem.* 2003; 14:1177. [PubMed: 14624632]
4. Guo H, Shenoy N, Gershman BM, Yang J, Sklar LA, Miao Y. *Nucl. Med. Biol.* 2009; 36:267. [PubMed: 19324272]
5. Yang J, Guo H, Miao Y. *Nucl. Med. Biol.* 2010; 37:873. [PubMed: 21055617]
6. Yang J, Miao Y. *Bioorg. Med. Chem. Lett.* 2012; 22:1541. [PubMed: 22297112]
7. Flook AM, Yang J, Miao Y. *Mol. Pharm.* 2013; 10:3417.
8. Flook AM, Yang J, Miao Y. *J. Med. Chem.* 2013 in press.
9. Chen J, Cheng Z, Hoffman TJ, Jurisson SS, Quinn TP. *Cancer Res.* 2000; 60:5649. [PubMed: 11059756]
10. Miao Y, Benwell K, Quinn TP. *J. Nucl. Med.* 2007; 48:73. [PubMed: 17204701]
11. Yang J, Miao Y. *Bioorg. Med. Chem.* 2010; 18:6695. [PubMed: 20728365]
12. Yang J, Guo H, Gallazzi F, Berwick M, Padilla RS, Miao Y. *Bioconjug. Chem.* 2009; 20:1634. [PubMed: 19552406]
13. **MC1 receptor binding affinity:** Amino acid and resin were purchased from Advanced ChemTech Inc. (Louisville, KY) and Novabiochem (San Diego, CA).  $^{125}\text{I}$ -Tyr<sup>2</sup>-[Nle<sup>4</sup>, D<sup>5</sup>Phe<sup>7</sup>]- $\alpha$ -MSH ( $^{125}\text{I}$ -Tyr<sup>2</sup>-NDP-MSH) was obtained from PerkinElmer, Inc. (Shelton, CT) for MC1 receptor binding assay. B16/F1 murine melanoma cells were obtained from American Type Culture Collection (Manassas, VA). The RAD-Arg-(Arg<sup>11</sup>)CCMSH was synthesized, purified by RP-HPLC and characterized by LC-mass spectroscopy according to our published procedure.<sup>11</sup> The IC<sub>50</sub> value of RAD-Arg-(Arg<sup>11</sup>)CCMSH for the MC1 receptor was determined in B16/F1 melanoma cells according to our published procedure.<sup>11</sup> Briefly, the B16/F1 cells ( $0.2 \times 10^6$  cells/well, n=3) were incubated at 25 °C for 2 h with approximately 30,000 counts per minute (cpm) of  $^{125}\text{I}$ -Tyr<sup>2</sup>-NDP-MSH in the presence of  $10^{-13}$  to  $10^{-6}$  M of RAD-Arg-(Arg<sup>11</sup>)CCMSH in 0.3 mL of binding medium. The IC<sub>50</sub> value of RAD-Arg-(Arg<sup>11</sup>)CCMSH was calculated using the Prism software (GraphPad Software, La Jolla, CA).
14. **Cellular internalization and efflux of  $^{99\text{m}}\text{Tc}$ -RAD-Arg-(Arg<sup>11</sup>)CCMSH:**  $^{99\text{m}}\text{TcO}_4^-$  was purchased from Cardinal Health (Albuquerque, NM) for peptide radiolabeling. All other chemicals used in this study were purchased from Thermo Fisher Scientific (Waltham, MA) and used without further purification. RAD-Arg-(Arg<sup>11</sup>)CCMSH was radiolabeled with  $^{99\text{m}}\text{Tc}$  using the method described previously.<sup>11</sup> The radiolabeled peptide was purified to single species by Waters RP-HPLC (Milford, MA) on a Grace Vydac C-18 reverse phase analytic column (Deerfield, IL) using a 20 min gradient of 16–26% acetonitrile in 20 mM HCl aqueous solution at a flow rate of 1 mL/min. Cellular internalization and efflux of  $^{99\text{m}}\text{Tc}$ -RAD-Arg-(Arg<sup>11</sup>)CCMSH were evaluated in B16/F1 melanoma cells according to our published procedure.<sup>11</sup>
15. **Biodistribution studies:** All the animal studies were conducted in compliance with Institutional Animal Care and Use Committee approval. The biodistribution of  $^{99\text{m}}\text{Tc}$ -RAD-Arg-(Arg<sup>11</sup>)CCMSH was determined in B16/F1 melanoma-bearing C57 mice (Harlan, Indianapolis, IN). C57 mice were subcutaneously inoculated on the right flank with  $1 \times 10^6$  B16/F1 cells. Tumor weights reached approximately 0.2 g at 10 days post cell inoculation. Each melanoma-bearing mouse was injected with 0.037 MBq of  $^{99\text{m}}\text{Tc}$ -RAD-Arg-(Arg<sup>11</sup>)CCMSH via the tail vein. Groups of 5 mice were sacrificed at 0.5, 2, 4 and 24 h post-injection, and tumors and organs of interest were harvested, weighed and counted. Blood values were taken as 6.5% of the whole-body weight. The specificity of tumor uptake was determined at 2 h post-injection by co-injecting  $^{99\text{m}}\text{Tc}$ -RAD-Arg-(Arg<sup>11</sup>)CCMSH with 10  $\mu\text{g}$  (6.1 nmol) of unlabeled NDP-MSH. Statistical analysis was performed using the Student's t-test for unpaired data to determine the significance of differences in tumor and kidney uptake between the groups in the biodistribution studies with/without peptide blockade. Differences at the 95% confidence level ( $p < 0.05$ ) were considered significant.

**16. Melanoma imaging and urinary metabolites of  $^{99m}\text{Tc}$ -RAD-Arg-(Arg<sup>11</sup>)CCMSH:**

Approximately 7.4 MBq of  $^{99m}\text{Tc}$ -RAD-Arg-(Arg<sup>11</sup>)CCMSH was injected in a B16/F1 melanoma-bearing C57 mouse for imaging and urine analysis. The mouse was euthanized at 2 h post-injection for small animal SPECT/CT (Nano-SPECT/CT<sup>®</sup>, Bioscan) imaging, as well as to collect urine for analyzing the metabolites. The 9-min CT imaging was immediately followed by the whole-body SPECT scan. The SPECT scans of 24 projections were acquired. Reconstructed SPECT and CT data were visualized and co-registered using InVivoScope (Bioscan, Washington DC). The collected urine sample was centrifuged at 16,000 g for 5 min before the HPLC analysis. Thereafter, aliquots of the urine were injected into the HPLC. A 20-minute gradient of 16–26% acetonitrile / 20 mM HCl with a flow rate of 1 mL/min was used for urine analysis.



## RAD-Arg-(Arg<sup>11</sup>)CCMSH

**Figure 1.**  
Schematic structure of RAD-Arg-(Arg<sup>11</sup>)CCMSH.

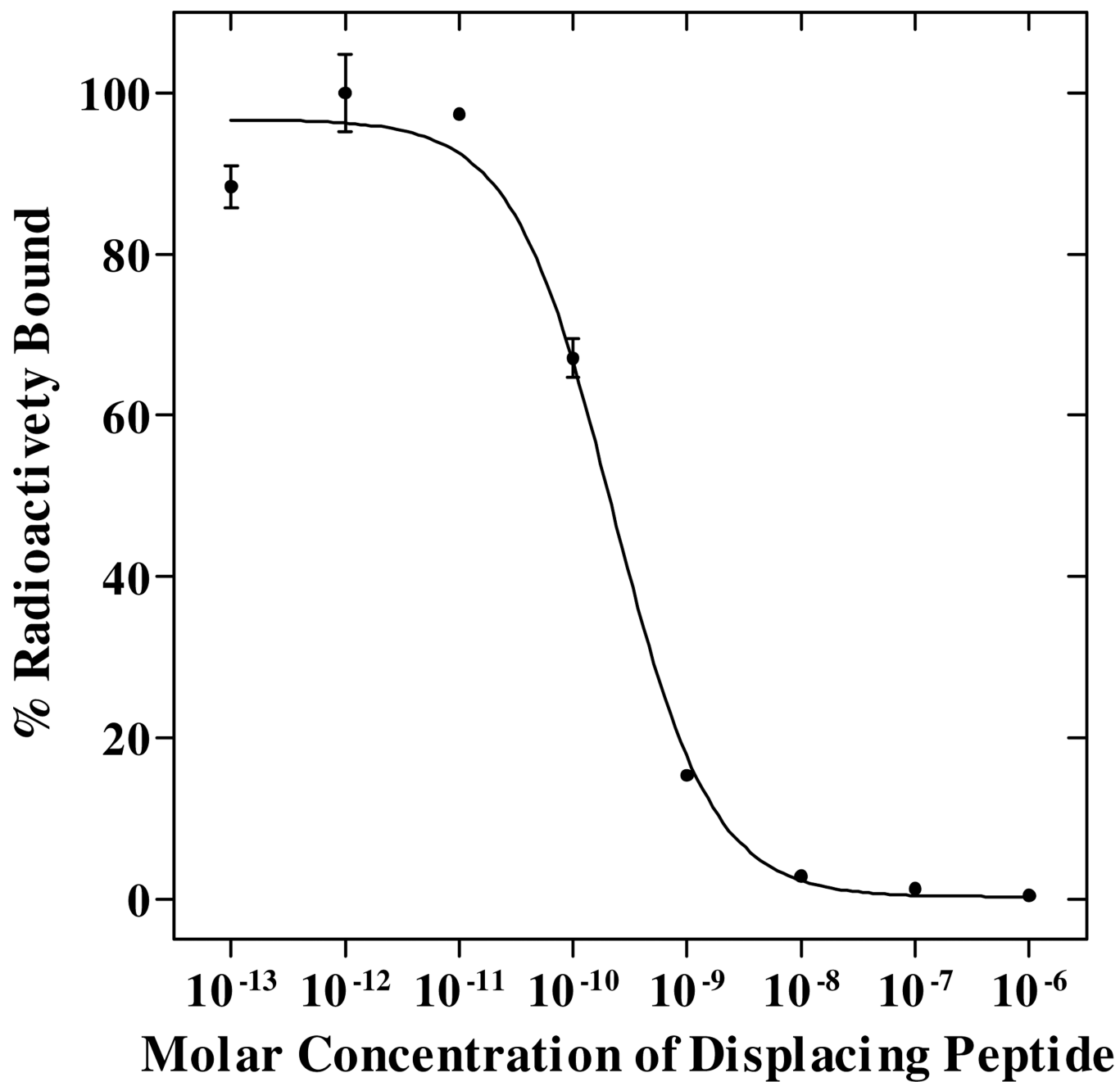


**Figure 2.**  
The competitive binding curve of RAD-Arg-(Arg<sup>11</sup>)CCMSH in B16/F1 melanoma cells.  
The IC<sub>50</sub> value of RAD-Arg-(Arg<sup>11</sup>)CCMSH was 0.22 nM.

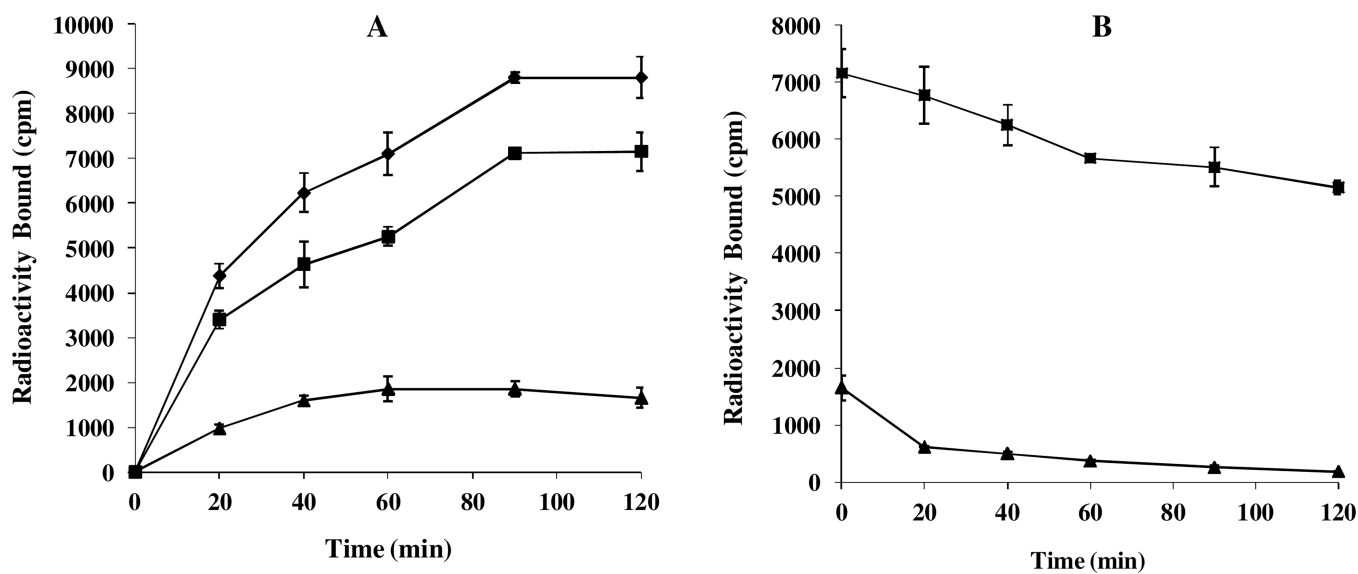


**Figure 3.** Cellular internalization (A) and efflux (B) of  $^{99m}\text{Tc}$ -RAD-Arg-(Arg<sup>11</sup>)CCMSH in B16/F1 melanoma cells. Total bound radioactivity (◆), internalized radioactivity (■) and cell membrane radioactivity (▲) were presented as counts per minute (cpm).



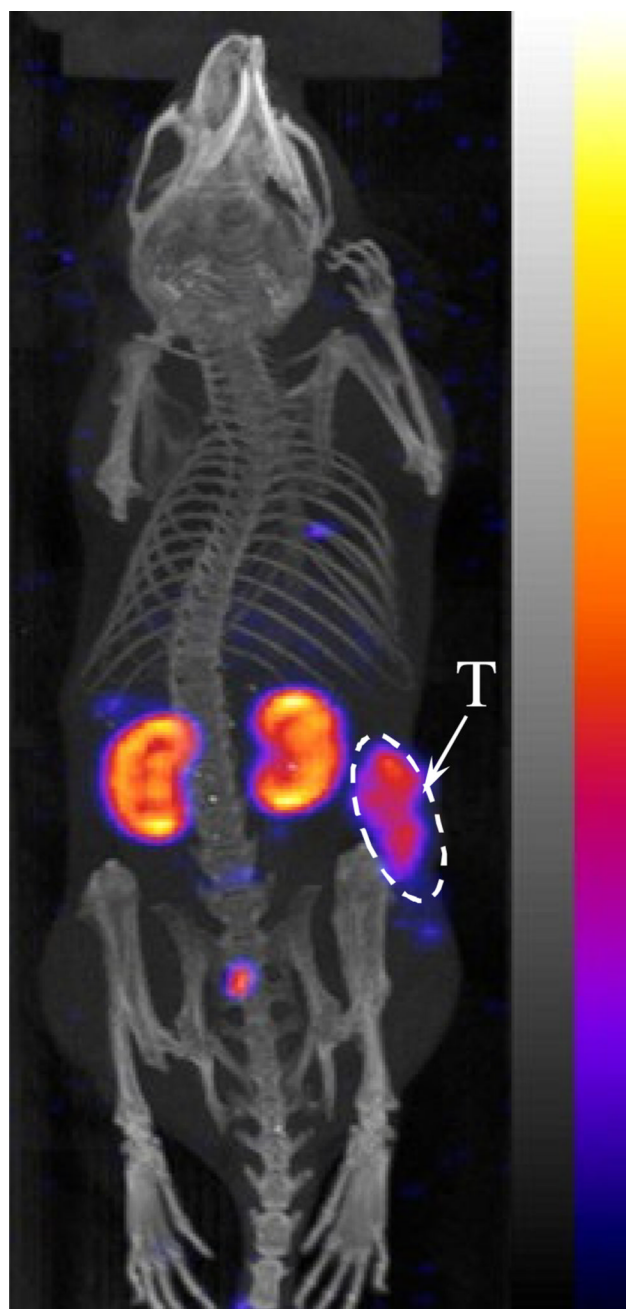


**Figure 4.** Representative whole-body SPECT/CT image of  $^{99m}\text{Tc}$ -RAD-Arg-(Arg<sup>11</sup>)CCMSH in a B16/F1 melanoma-bearing C57 mouse at 2 h post-injection. Flank melanoma lesions (T) are highlighted with an arrow on the images.

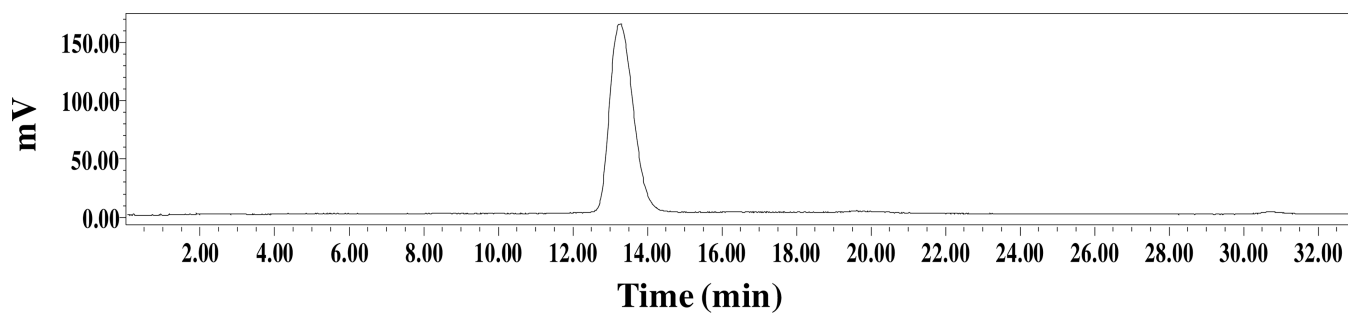


**Figure 5.** Radioactive HPLC profile of urine sample of a B16/F1 melanoma-bearing C57 mouse at 2 h post-injection of  $^{99m}\text{Tc}$ -RAD-Arg-(Arg<sup>11</sup>)CCMSH. The retention time (13.3 min) of the original compound of  $^{99m}\text{Tc}$ -RAD-Arg-(Arg<sup>11</sup>)CCMSH prior to the tail vein injection is identical with that of the urine sample of  $^{99m}\text{Tc}$ -RAD-Arg-(Arg<sup>11</sup>)CCMSH.

Biodistribution of  $^{99m}\text{Tc}$ -RAD-Arg-(Arg<sup>11</sup>)CCMSH in B16/F1 melanoma-bearing C57 mice. The data was presented as percent injected dose/gram or as percent injected dose (mean $\pm$ SD, n=5)

Table 1

Tissue	0.5 h	2 h	4 h	24 h	2 h NDP blockade
Percent injected dose/gram (%ID/g)					
Tumor	8.46 $\pm$ 3.70	17.98 $\pm$ 4.96	14.07 $\pm$ 2.90	10.16 $\pm$ 2.66	2.39 $\pm$ 0.66*
Brain	0.16 $\pm$ 0.04	0.04 $\pm$ 0.02	0.02 $\pm$ 0.02	0.02 $\pm$ 0.00	0.06 $\pm$ 0.02
Blood	3.43 $\pm$ 0.37	0.59 $\pm$ 0.17	0.10 $\pm$ 0.06	0.04 $\pm$ 0.01	0.99 $\pm$ 0.05
Heart	1.71 $\pm$ 0.58	0.50 $\pm$ 0.14	0.21 $\pm$ 0.03	0.10 $\pm$ 0.02	0.66 $\pm$ 0.12
Lung	5.42 $\pm$ 0.70	1.15 $\pm$ 0.22	0.40 $\pm$ 0.16	0.16 $\pm$ 0.03	1.38 $\pm$ 0.49
Liver	3.07 $\pm$ 0.08	1.88 $\pm$ 0.35	1.47 $\pm$ 0.11	1.18 $\pm$ 0.28	2.13 $\pm$ 0.27
Skin	5.43 $\pm$ 0.41	1.10 $\pm$ 0.39	0.53 $\pm$ 0.09	0.24 $\pm$ 0.10	1.15 $\pm$ 0.20
Spleen	2.12 $\pm$ 0.57	0.61 $\pm$ 0.31	0.25 $\pm$ 0.12	0.41 $\pm$ 0.14	0.84 $\pm$ 0.36
Stomach	3.13 $\pm$ 0.62	1.63 $\pm$ 0.43	1.41 $\pm$ 0.74	0.28 $\pm$ 0.09	2.35 $\pm$ 0.61
Kidneys	41.24 $\pm$ 4.48	35.64 $\pm$ 9.61	26.51 $\pm$ 0.62	11.99 $\pm$ 2.29	27.16 $\pm$ 5.58
Muscle	0.80 $\pm$ 0.46	0.20 $\pm$ 0.15	0.15 $\pm$ 0.10	0.03 $\pm$ 0.02	0.23 $\pm$ 0.07
Pancreas	1.06 $\pm$ 0.33	0.20 $\pm$ 0.11	0.10 $\pm$ 0.05	0.10 $\pm$ 0.05	0.29 $\pm$ 0.10
Bone	1.97 $\pm$ 0.22	0.64 $\pm$ 0.25	0.34 $\pm$ 0.13	0.14 $\pm$ 0.04	0.92 $\pm$ 0.26
Percent injected dose (%ID)					
Intestines	2.53 $\pm$ 0.18	1.38 $\pm$ 0.41	2.24 $\pm$ 1.08	0.41 $\pm$ 0.11	2.50 $\pm$ 0.16
Bladder	46.28 $\pm$ 2.59	74.50 $\pm$ 7.30	80.16 $\pm$ 2.77	91.45 $\pm$ 1.86	77.85 $\pm$ 2.34
Uptake Ratio of Tumor/Normal Tissue					
Tumor/Blood	2.47	30.47	140.70	254.00	2.41
Tumor/Kidneys	0.21	0.50	0.53	0.85	0.09
Tumor/Lung	1.56	15.63	35.18	63.50	1.73
Tumor/Liver	2.76	9.56	9.57	8.61	1.12
Tumor/Muscle	10.58	89.90	93.80	338.67	10.39

\* p<0.05 (p=0.00006), significance comparison in tumor and kidney between  $^{99m}\text{Tc}$ -RAD-Arg-(Arg<sup>11</sup>)CCMSH with/without peptide blockade at 2 h post-injection.